

Light Transmission Measurements in Solid Fuel Ramjet Combustors

Michael E. Hewett* and David W. Netzer†
Naval Postgraduate School, Monterey, Calif.

An experimental investigation of the combustion behavior in solid fuel ramjets was conducted using polymethylmethacrylate fuel grains. Multiple wavelength light transmission measurements were made at the fuel grain exit and nozzle entrance to study the effects of bypass ratio on the combustion efficiency and the percentage and size of unburned carbon. Utility and limitations of the optical method are presented. Combustion efficiency did not correlate with the percentage of unburned carbon. Unburned hydrocarbons were the apparent cause of combustion inefficiency. Fuel regression rate and combustion efficiency were also found to be sensitive to small variations in fuel manufacturing methods.

Nomenclature

A/F	= air-fuel ratio on mass basis
C_m	= mass concentration of particles, kg particulates/m ³ gas
D_{32}	= volume to surface mean diameter, m
G	= air mass flux, kg/m ² -s
L	= length of path through aerosol, m
\dot{m}	= flow rate, kg/s
P	= pressure, N/m ²
\bar{Q}	= average extinction coefficient
\dot{r}	= fuel regression rate, m/s
T	= fraction of light transmitted
γ	= turbidity
$\eta_{\Delta T}$	= temperature rise combustion efficiency
ρ	= particulate density, kg/m ³
σ	= standard deviation

Introduction

A BETTER understanding of the internal ballistics of the solid fuel ramjet continues to be a necessary goal, if the concept is to become a viable tactical propulsion system.

Past studies^{1,2} have shown the importance of parameters such as flame holder step size, aft mixing chamber entrance step size and length to diameter ratio, and aft mixing techniques.

Mady et al.³ conducted an investigation in which the effects of bypass air on combustion efficiency were studied. In that investigation bypass mass flow rates, dump momentum, the number of dumps, and angular orientation into the aft mixing chamber were varied. With bypass (low mass flux through the fuel port) and polymethylmethacrylate (PMM) fuel grains it was found that the regression rate did not vary with air mass flux. The regression rate for bypass configurations took the form

$$\dot{r} = 7.15 \times 10^{-5} p^{0.42} \quad [p = (3.2 \rightarrow 3.8) \times 10^5] \quad (1)$$

It was suggested that in the bypass configuration (low G , high P , and fuel rich within the fuel port) the principal mechanism for wall heat flux became radiation and thus the regression rate was insensitive to G .

For the nonbypass configuration, port air-fuel ratios were generally lean and the regression rates took the form

$$\dot{r} = 6.97 \times 10^{-5} p^{0.29} G^{0.38} \quad \begin{matrix} [P = (2 \rightarrow 4.5) \times 10^5] \\ [G = 70 \rightarrow 140] \end{matrix} \quad (2)$$

Experimental data showed a significant decrease in combustion efficiency for all bypass configurations that were used. It was concluded that the monomer/small polymer and/or carbon that entered the aft mixing chamber would react most completely if allowed to mix slowly with the hot core gases. Bypass air apparently quenched these reactions within the reacting shear layer downstream of the fuel grain.

Work at the Naval Weapons Center, China Lake, and at the Chemical Systems Division, United Technologies (CSD) have shown that when all-hydrocarbon fuel grains are used in the solid fuel ramjet, combustion efficiency can be improved with the use of bypass air. These fuels characteristically have higher regression rates than PMM and much of the fuel probably leaves the fuel surface as large polymers. Apparently the unburned hydrocarbons/carbon are hot enough and the fuel port flow rich enough that bypass air can increase the reaction rates within the aft mixing chamber.

Additional experimental work by Schadow¹ with all-hydrocarbon fuels, and modeling efforts by Netzer⁴ and by Dunlap² have indicated that a considerable amount of unburned carbon and/or hydrocarbons are present at the aft end of the fuel grain. It also has been suggested that combustion efficiency losses result from the unburned carbon. Except for the gas sampling and temperature measurements made by Schadow, no direct measurements of the gas/solid composition leaving the fuel grain have been made.

In recent years considerable advances have been made in the utilization of light transmission and light scattering methods^{5,6} for the study of combustion behavior. Cashdollar et al.⁷ have employed an optical transmissometer for measuring carbon particle size and concentration in a wood tunnel fire. Lester and Wittig⁸ successfully utilized the light transmission method to find particle sizes and concentration during methane combustion in a shock tube. Powell et al.⁹ utilized both transmission and angular scattering of light methods to study smoke particles in building fires. Although the latter method negates the requirement for a priori knowledge of the refractive index of the particles, it is more difficult to adapt to practical combustion chamber geometries. Bernard and Penner¹⁰ have also used scattered laser power spectra to determine particle sizes in flames.

This investigation was concerned with further study of the combustion process within solid fuel ramjets. Unburned

Submitted May 29, 1980; revision received Oct. 28, 1980. This paper is declared a work of the U.S. Government and is therefore in the public domain.

*LCDR, U.S. Navy.

†Associate Professor, Department of Aeronautics. Member AIAA.

carbon particle sizes and concentrations were determined in the aft mixing chamber, both at the fuel grain exit and just prior to the exhaust nozzle. The optical technique employed involved the light transmission method as utilized by Cashdollar et al.⁷

Method of Investigation

Experimental firings of a solid fuel ramjet were conducted using PMM fuel grains and several different bypass air flow ratios. A schematic of the test apparatus is shown in Fig. 1. Continuous measurements of light transmission were made at two positions in the aft mixing chamber (Fig. 2).

The transmission measurements record the total amount of light removed from the beam passing through the combustion chamber as a result of the scattering and absorption by the particulates. The transmission of light through an aerosol of particles is given by Bouguer's Law¹¹

$$T = e^{-\gamma L} \quad (3)$$

The intensity of the light beam decreases exponentially with distance (L) as it penetrates the aerosol, with a rate of decay regulated by the turbidity γ . The turbidity for the case of a polydispersed size distribution is given by⁷

$$\gamma = \frac{3}{2} \frac{\bar{Q} C_m}{D_{32} \rho} \quad (4)$$

The average extinction coefficient \bar{Q} is calculated as a function of particle size distribution, wavelength of the light beam, and the complex refractive index of the particle using Mie scattering theory. Values of \bar{Q} have been shown not to be significantly affected when the particles are nonspherical.⁷

The actual values of the refractive index and the particle size distribution of the carbon particles generated within the solid fuel ramjet are not known. The refractive index likely varies somewhat with fuel composition⁸ and operating conditions (pressure, air flow rate, etc.). Values used for carbon/soot generated in various flames are presented in Refs. 8, 12, and 13. A brief review of the available data has been presented by Cashdollar et al.⁷ In this investigation values of $1.95-0.66i$, $1.80-0.60i$, and $1.80-0.30i$ were employed. Various particle size distributions including monodispersed and log normal have been reported^{8,14} depending upon the fuel composition and test environment.

Average extinction coefficients as a function of particle diameter were calculated for the aforementioned indices of

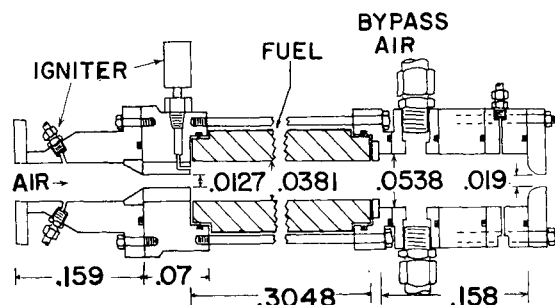


Fig. 1 Schematic of solid fuel ramjet.

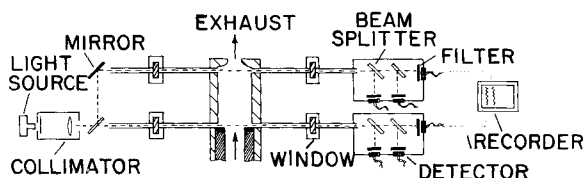


Fig. 2 Schematic of optical detector.

refraction for monodispersed particles as well as for log normal particle size distributions with standard deviations of 1.5 and 2.0. These curves were generated using a Mie scattering computer code provided by K.L. Cashdollar. Typical curves are presented in Fig. 3 for wavelengths of 4500, 5145, and 6328 Å.

From Bouguer's Law⁷ the ratio of the logarithms of the measured transmissions at any two wavelengths is equal to the ratio of the computed average extinction coefficients.

$$\frac{\ln T_{\lambda_1}}{\ln T_{\lambda_2}} = \frac{\bar{Q}_{\lambda_1}}{\bar{Q}_{\lambda_2}} \quad (5)$$

Curves from which average particle size can be found as a function of the \bar{Q} ratios are shown in Fig. 4.

As noted by Cashdollar,⁷ use of three wavelengths provides a redundancy over most of the particle size range. If the three measured log transmission ratios do not yield the same approximate average particle diameter, then the particle size distribution width σ and/or the refractive index is not correct. This was the reason for generating multiple sets of plots for different indices of refraction and size distributions.

Once the mean particle size and extinction coefficient have been determined, the mass concentration can then be computed from

$$C_m = -\frac{2}{3} [(\rho D_{32}) / (\bar{Q}_\lambda L)] \ln T_\lambda \quad (6)$$

provided that the particle density is known.

Cashdollar used light wavelengths of 4500, 6328, and 10,000 Å. The wide spread in wavelength increases the accuracy of the technique.^{6,7} However, in applying the technique to flame measurements, light emission in the infrared region of 10,000 Å makes this frequency unusable. For

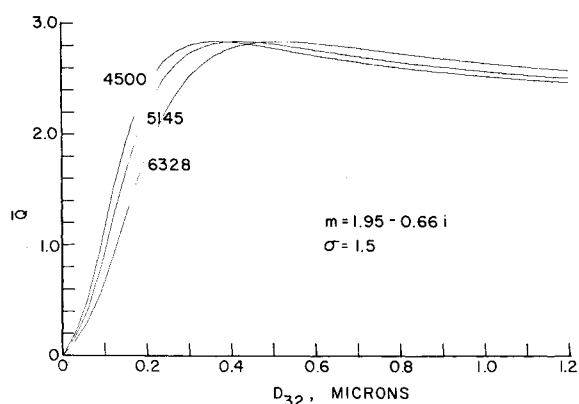


Fig. 3 Average extinction coefficients.

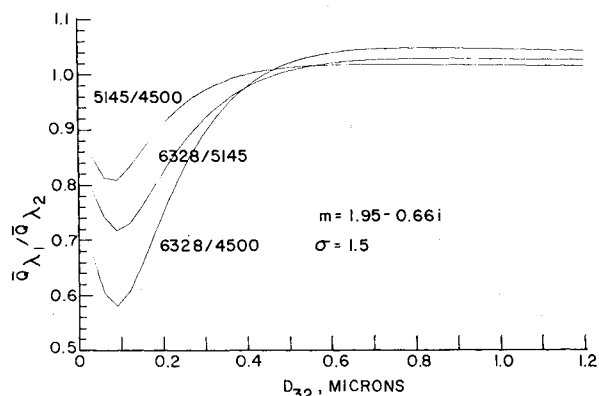


Fig. 4 Average extinction coefficient ratios.

the solid fuel ramjet combustion studied in this investigation 5145 Å was used rather than 10,000 Å. However, it offered less in the way of redundancy for the measurement as it was closer to the other frequencies than desired.

Description of Apparatus

The solid fuel ramjet motor was that previously used by Mady.³ The only modifications made to the motor were the installation of an improved ethylene-oxygen igniter system in the head-end assembly and the machining of 0.0143 m diam ports in the aft mixing chamber. The ports allowed an external light source to penetrate through the aft mixing chamber at two axial locations (Fig. 2). Fuel grains used were fabricated from 0.1016 m thick sheets of cast plexiglass.

The light source used was a SLM-1200 slide projector which housed a 1200 W tungsten-halogen lamp (Sylvania BRN-1200). The light was focused through the projector lens system onto a pin hole. The pin hole produced a nearly point source illumination and was used with a collimating lens to produce a collimated light beam.

The beam was then split with a 50/50 plate beam splitter. The first beam was directed to the front portion of the mixing chamber. The second beam was directed to the aft end of the mixing chamber just prior to the exhaust nozzle. After both beams penetrated the chamber cavity they were again directed through tubing to two individual light detector units.

The distance traveled by the light beam through the tubing, prior to reaching the light detector, was nominally 0.61 m. This limited the angular field of view of the detector to 1.1 deg in order to eliminate any significant forward light scattering.⁷

Each detector box consisted of two plate beam splitters which created three individual beams of light (Fig. 2). 0.051 × 0.051 m narrow pass light filters of wavelengths 6328, 5145, and 4500 Å were placed directly in front of three silicon photovoltaic detectors. The detectors provided adequate spectral response between 2000 and 11,500 Å. The output of each photodetector was input to an operational amplifier, providing linearity between light intensity and voltage output.

Experimental Procedure

All test firings were performed in the jet engine test cell at the Naval Postgraduate School.

Firings were made at bypass ratios (primary/bypass) of 100/0, 70/30, 50/50 and 30/70, with a nominal total air mass flow rate of 0.0907 kg/s. Reduced mass flow rates of 0.0454 kg/s with no bypass were also tested. Bypass dump diameters of 0.0207 and 0.0063 m were employed.

Temperature rise efficiencies were calculated for each test. Inlet temperatures were measured and "actual" combustor stagnation temperature was calculated using measured flow rates and combustion pressure. The NWC PEPCODE program was used to generate the theoretical combustion temperature and required gas properties (gas constant and specified heat ratio) at the experimentally determined air-fuel ratio.

Weighing each fuel grain before and after a firing provided the needed data for determining the average fuel regression rate and fuel mass flow rate \dot{m}_f .

Results and Discussion

Transmissivity measurements were successful with both front and back light detector systems at 100/0 and 70/30 bypass ratios. When operating at 50/50 or 30/70, however, the light transmission during steady-state burning through the front portion of the mixing chamber was below the sensitivity of the recording system. Light transmission was always measurable in the aft end of the mixing chamber. For each test, the available data were used to calculate log-transmission ratios ($\ln T_{6328}/\ln T_{4500}$, $\ln T_{6328}/\ln T_{5145}$, and $\ln T_{5145}/\ln T_{4500}$) at 16 and 26 s into the firing. Extinction coefficient ratio curves (Fig. 4) for $\sigma = 1.5$ and 2.0 and monodispersed, and for in-

dices of refraction of 1.95-0.66i, 1.80-0.60i and 1.80-0.30i were employed to find D_{32} . The most consistent agreements in predicted D_{32} values for the three log-transmission ratios resulted from a monodispersed distribution and a log-normal distribution with index of refraction equal to 1.95-0.66i. As mentioned earlier the required narrow range of wavelengths limited the accuracy of the technique when applied to the solid fuel ramjet. D_{32} predictions were often consistent within 0.02 microns but at times disagreed by as much as 0.06 μm from a mean diameter of approximately 0.20 μm . However, the attempt in this investigation was only to obtain approximate particle sizes and concentrations so that relative effects of motor operating conditions could be evaluated.

Test firings with no bypass (100/0) indicated that the regression rate varied within 3% (except for one test) of Eq. (2). The results were also within 6% of the regression rate results presented by Boaz and Netzer¹⁵

$$\dot{r} = 3.69 \times 10^{-6} P^{0.51} G^{0.41} \quad \begin{matrix} [P = (2.5-7.5) \times 10^5] \\ [G = 45-172] \end{matrix} \quad (7)$$

With application of bypass air (decreased G) the regression rates decreased in accordance with Eq. (2). This was opposite to the findings of Mady where regression rates did not vary significantly with bypass and no longer followed Eq. (2).

The computed combustion efficiencies showed (in contrast to Mady's experiments) no degradation in performance with bypass air (see Fig. 5).

The contradictory results prompted an investigation of possible differences in the PMM fuel and/or in test procedures. All air mass flow measurement orifices were recalibrated and found to be accurate. Samples of PMM used in both experiments were accurately measured for possible differences in density and found equal. Information received from the PMM manufacturer (Rohm and Haas) indicated a possible difference in lots of PMM due to the curing process. It was suggested that when curing thick sections of PMM a possible variation in the amount of residual monomer in the solid may occur. Subsequently, a sample of each lot was ignited in atmospheric air with an oxygen-acetylene torch and a significant difference in the surface combustion was apparent. The sample used in this experiment appeared to have a considerable fizz layer on the surface, indicating the probable existence of large quantities of monomers leaving in a gaseous state. The sample from the earlier experiments, although showing some surface fizz, produced large gas bubbles well below a relatively smooth combustion surface.

With the assumption that the previously employed fuel came off the surface predominately as small polymers rather than monomers, a plausible explanation for the higher regression rates in the bypass run can be made. For a low mass

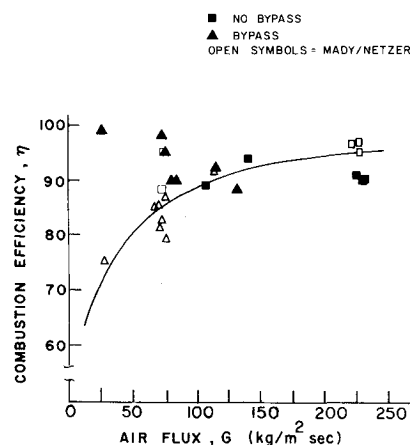


Fig. 5 Temperature rise combustion efficiency.

Table 1 Summary of primary experimental results ($T_{\text{air}} = 290 \text{ K}$)

% Primary/% bypass		100%/0%				70%/30%
Run	1	2	3	4	5	6
$P_c \times 10^{-5}, N/m^2$	3.77	2.46	2.69	3.75	3.85	3.31
$\dot{r} \times 10^3, m/s$	0.150	0.108	0.108	0.149	0.158	0.119
$\dot{m}_{\text{primary}}, kg/s$	0.0921	0.0558	0.0658	0.0903	0.0921	0.0635
$\dot{m}_{\text{bypass}}, kg/s$	0	0	0	0	0	0.0272
A/F	12.2	10.6	12.4	13.0	11.7	15.6
$(A/F)_{\text{fuel port}}$	12.2	10.6	12.4	13.0	11.7	10.9
$\eta_{\Delta T}$	0.90	0.89	0.94	0.91	0.90	0.88
$T_{\text{front}}(6328)^b$	0.57	0.78	0.70	0.74	0.71	0.46
$T_{\text{back}}(6328)^b$	0.94	0.87	0.97	0.79	0.84	0.71
$D_{32\text{front}}, \mu m^c$	0.20	0.18	0.15	0.2	0.17	0.15
$D_{32\text{back}}, \mu m^c$	0.14	0.45	—	0.17	—	0.27
$C_{m\text{front}}, kg/m^3$	1.67×10^{-3}	7.48×10^{-4}	1.14×10^{-3}	8.9×10^{-4}	1.04×10^{-3}	2.49×10^{-3}
$C_{m\text{back}}, kg/m^3$	2.76×10^{-4}	5.99×10^{-4}	—	7.15×10^{-4}	—	1.04×10^{-3}
Unburned carbon %						
Front	4.7	3.2	4.9	2.5	2.80	8.5
Back	0.7	2.6	—	2.0	—	3.5

		50%/50%				30%/70%
Run	7	8	9 ^a	10	11	12
$P_c \times 10^{-5}, N/m^2$	4.06	3.27	3.27	3.27	3.27	3.21
$\dot{r} \times 10^3, m/s$	0.128	0.107	0.104	0.106	0.109	0.075
$\dot{m}_{\text{primary}}, kg/s$	0.0581	0.0485	0.0463	0.0481	0.0454	0.0318
$\dot{m}_{\text{bypass}}, kg/s$	0.0594	0.0454	0.0467	0.0467	0.0458	0.0590
A/F	18.8	18.2	18.3	18.5	17.0	20.4
$(A/F)_{\text{fuel port}}$	9.4	9.11	9.15	9.25	8.5	6.12
$\eta_{\Delta T}$	0.92	0.90	0.95	0.90	0.98	0.99
$T_{\text{front}}(6328)^b$	0	0	0	0	0	0
$T_{\text{back}}(6328)^b$	0.65	0.66	0.59	—	0.56	0.68
$D_{32\text{front}}, \mu m^c$	—	—	—	—	—	—
$D_{32\text{back}}, \mu m^c$	0.265	0.22	0.23	—	0.30	0.17
$C_{m\text{front}}, kg/m^3$	—	—	—	—	—	—
$C_{m\text{back}}, kg/m^3$	1.27×10^{-3}	1.22×10^{-3}	1.56×10^{-3}	—	1.86×10^{-3}	1.45×10^{-3}
Unburned carbon, %						
Front	—	—	—	—	—	—
Back	3.9	4.5	6	—	7.0	6.2

^a High bypass damp momentum. ^b Transmittance at $t_{\text{ign}} + 16 \text{ s}$, total burn time $\sim 40 \text{ s}$. ^c Calculated from 6328/4500 for $\sigma = 1.5$.

flux of air through the grain, as for 50/50 bypass, a fuel rich condition occurred. A high concentration of fuel polymers reaching the flame would lead to cracking and the production of increased quantities of free carbon. The increased presence of carbon would enhance radiative heat transfer to the fuel surface, increasing the regression rate.

With the high regression rate and resulting fuel rich environment, the temperatures in Mady's experiments must have been low enough and/or the combustion shear zone thin enough that when bypass air was injected into the aft mixing chamber the combustion process was quenched.

In the current experiments, if monomer production predominated, the reactions would be more rapid and complete and less carbon would be produced by cracking type processes below the flame zone. Less radiative heat transfer would result, with correspondingly lower fuel regression rates. The low regression rate resulted in near stoichiometric air-fuel ratios within the fuel grain with 50/50 bypass. The bypass air would then mix with the hotter combustion products that included only relatively small quantities of unburned fuel. The subsequent reactions apparently occurred without quenching, resulting in high combustion efficiencies.

Light transmission measurements for no-bypass (high G through fuel grain) showed greater than 70% transmittance (except for one test) at the end of the fuel grain and greater

Table 2 Estimated average percentage of unburned carbon

Estimated % unburned carbon		% Air (fuel port/bypass)	$\eta_{\Delta T}$
Forward	Aft		
3.3	1.4	100/0	0.90
4.0	2.6	100/0 (low G)	0.91
8.5	3.5	70/30	0.88
>30	5.3	50/50	0.94
>30	6.2	30/70	0.99

than 79% transmittance at the entrance to the nozzle. This indicated that only small quantities of particulates left the fuel port. Assuming for simplicity that the gas properties and carbon concentration are uniform at any cross section of the aft mixing chamber, the percentage of unburned carbon can be estimated. It varies linearly with particulate concentration and gas velocity and inversely with the fuel flow rate. This assumption is obviously weak at the end of the grain where reverse flow occurs in the recirculation region. Major experimental data are presented in Table 1. Table 2 presents the estimated average percentage of unburned carbon for each of

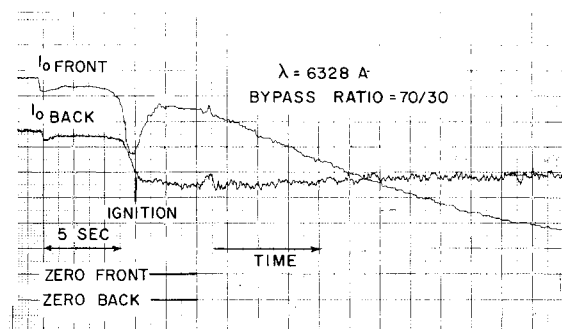


Fig. 6 Light transmission data.

the test conditions. Figure 6 presents typical light transmission data.

Without bypass, reducing air flow rate decreased the air-fuel ratio slightly as expected from the behavior of the fuel regression rate. However, the air-fuel ratio remained air rich (stoichiometric $A/F = 8.33$). The combustion efficiency and the percentage of unburned carbon did not vary appreciably.

With bypass ratios up to 50/50 the air-fuel ratio within the fuel port remained air rich. However, for 50/50 bypass conditions the fuel port air-fuel ratio was nearly stoichiometric. In the 50/50 bypass configuration transmittance at the fuel grain exit was less than 5%. This was considered the minimum measurable transmittance level for the present system. This indicated that greater than 30% of the carbon produced was unburned leaving the fuel grain (or rather leaving the fuel grain and trapped in the recirculation zone). Thus, even with near stoichiometric mixture ratios within the fuel port, a considerable amount of unburned carbon was produced. With the higher regression rates obtained by Mady's experiments, excessive amounts of carbon must have been produced. As the percentage bypass air was increased, more carbon was produced within the fuel grain and more passed through the nozzle. Much of the increased carbon content within the fuel grain was apparently burned in the aft mixing chamber. This is also apparent in Fig. 6; as the grain continued to burn, the port mixture became less fuel lean and more carbon was produced, yet the percentage of unburned carbon at the exhaust nozzle remained approximately constant. The combustion efficiency did not change appreciably although a slight increase was noted with increasing bypass ratio to the 50/50 conditions. The high bypass condition (30/70) was the only test conducted in which the air-fuel ratio within the fuel port was fuel rich and it provided the highest overall air-fuel ratio and combustion efficiency.

For the combustion of PMM with air, 1% unburned carbon would reduce combustion efficiency by approximately 1% (if fuel lean and with chemical equilibrium).

The results presented in Tables 1 and 2 indicate that a small amount of unburned carbon in itself is not the cause for low combustion efficiency. Rather, it appears in this case that unburned gaseous hydrocarbons have the primary effect on combustion efficiency. Port air-fuel ratios close to stoichiometric (or slightly fuel rich) produce thicker boundary layers (higher fuel regression rates relative to air flow rates). This in turn results in a thicker fuel shear layer entering the aft mixing chamber with more unburned hydrocarbons at a higher temperature. When these hydrocarbons are small (monomers, etc.) they apparently burn quite efficiently with the bypass air (or for that matter without bypass air). If the fuel leaving the surface is in larger polymers (as for the fuel-rich bypass conditions in Mady's experiments), more carbon is produced and apparently the aft mixing process becomes much more critical. The temperature of the larger polymers and the carbon become important and how the bypass air is mixed becomes the dominant variable affecting combustion efficiency.

These results indicate that fuels which could produce gaseous monomers may provide a high performing solid fuel ramjet without the complexity of bypass if adequate fuel regression rates are obtained to provide only slightly air rich mixture ratios and adequate mixing occurs to allow complete combustion.

The percentage of unburned carbon was determined from the computed carbon concentration C_m , which in turn was determined from the transmissometer readings. The calculated particle sizes were in the $0.1\text{--}0.25\text{ }\mu\text{m}$ range. This agreed with carbon particle size measurements in flames and smoke made by other investigators. In any case, a variation in particle diameter between 0.1 and $0.3\text{ }\mu\text{m}$ does not significantly affect C_m since in this range \bar{Q} varies in an approximately linear manner with particle diameter D_{32} . This can be seen from the equation for particle mass concentration

$$C_m = [-2/3(\rho D_{32}) / (\bar{Q}L)] \ln T$$

One of the more interesting results of these experiments was the unexpected change in bypass performance compared to the earlier data for PMM.³ The apparent production of monomers enhanced bypass combustion efficiency but reduced regression rate by significantly reducing the radiation produced by carbon particles. These differences apparently resulted from small variations in manufacturing methods. These observations indicate that the often observed run-to-run variations in combustion efficiency may be due in part to small variations in the fuel curing process.

Conclusions

The three-wavelength light transmission technique provided an approximate method for evaluating the effects of motor operating environment on particulate levels and combustion efficiency.

The amounts of unburned carbon leaving the fuel grain and/or entering the nozzle did not correlate with combustion efficiency. Unburned gaseous hydrocarbons were apparently the primary cause of combustion inefficiency.

The results indicate the desirability of fuels that unzip to produce monomers. These type fuels may provide high combustion efficiency without the complexity of bypass; if adequate fuel-air ratios can be maintained and sufficient mixing occurs.

Small variations in fuel manufacturing methods were found to significantly effect the obtainable combustion efficiency of PMM.

Acknowledgment

This work was sponsored by the Naval Weapons Center, China Lake, Calif.

References

- ¹Schadow, K.C., Cordes, H.F., and Chieze, P.J., "Experimental Studies of Combustion Processes in Solid Fuel Ramjets," presented at 13th JANNAF Combustion Meeting, Monterey, Calif., Sept. 1976.
- ²Jensen, G.E., Dunlap, R., and Holzman, A.L., "Solid Fuel Ramjet Flame Stabilization and Fuel Regression Studies," presented at 12th JANNAF Combustion Meeting, Newport, R.I., Aug. 1975.
- ³Mady, C.J., Hickey, P.H., and Netzer, D.W., "Combustion Behavior of Solid Fuel Ramjets," *Journal of Spacecraft and Rockets*, Vol. 15, May-June 1978, pp. 131-132.
- ⁴Netzer, D.W., "Model Applications to Solid-Fuel Ramjet Combustion," *Journal of Spacecraft and Rockets*, Vol. 15, Sept.-Oct. 1978, pp. 263-264.
- ⁵Dobbins, R.A. and Jizmagian, G.S., "Particle Size Measurements Based on Use of Mean Scattering Cross Sections," *Journal of the Optical Society of America*, Vol. 56, Oct. 1966, pp. 1351-1354.
- ⁶Dobbins, R.A. and Jizmagian, G.S., "Optical Scattering Cross Sections for Polydispersions of Dielectric Spheres," *Journal of the Optical Society of America*, Vol. 56, Oct. 1966, pp. 1345-1350.

⁷Cashdollar, K.L., Lee, C.K., and Singer, J.M., "Three-Wavelength Light Transmission Technique to Measure Smoke, Particle Size and Concentration," *Applied Optics*, Vol. 18, June 1979, pp. 1763-1769.

⁸Lester, T.W. and Wittig, S.L.K., "Particle Growth and Concentration Measurements in Sooting Homogeneous Hydrocarbon Combustion Systems," *Modern Developments in Shock Tube Research*, 10th International Shock Tube Symposium, NTIS, 1975, pp. 632-639.

⁹Powell, E.A., Cassanova, R.A., Bankston, C.P., and Zinn, B.T., "Smoke Diagnostics by Means of Optical Measurement Techniques," AIAA Paper 67-76, presented at AIAA 14th Aerospace Sciences Meeting, Jan. 26-28, 1976.

¹⁰Bernard, J.M. and Penner, S.S., "Determination of Particle Sizes in Flames from Scattered Laser Power Spectra," AIAA Paper

76-207, presented at AIAA 14th Aerospace Sciences Meeting, Jan. 26-28, 1976.

¹¹Jenkins, F.A. and White, H.E., *Fundamentals of Optics*, McGraw-Hill, 1957, p. 200.

¹²Senftleben, H. and Benedict, E., *Annalen Der Physik*, Über die optischen Konstanten und die strahlungs gesetze der Kohle, Vol. 54, No. 17, 1917, p. 65.

¹³Dalzell, W.H. and Sarofim, A.F., *Journal of Heat Transfer*, Über die optischen Konstanten und die strahlung sgesetze der Kohle, Vol. 91, 1969, pp. 100-104.

¹⁴Wersborg, B.L., "Physical Mechanisms of Carbon Formation in Flames," Thesis, M.I.T., Cambridge, Mass., 1972.

¹⁵Boaz, L.D. and Netzer, D.W., "An Investigation of the Internal Ballistics of Solid Fuel Ramjets," Naval Postgraduate School Rept. 57Nt73031A, March 1973.

From the AIAA Progress in Astronautics and Aeronautics Series...

ENTRY HEATING AND THERMAL PROTECTION—v. 69

HEAT TRANSFER, THERMAL CONTROL, AND HEAT PIPES—v. 70

Edited by Walter B. Olstad, NASA Headquarters

The era of space exploration and utilization that we are witnessing today could not have become reality without a host of evolutionary and even revolutionary advances in many technical areas. Thermophysics is certainly no exception. In fact, the interdisciplinary field of thermophysics plays a significant role in the life cycle of all space missions from launch, through operation in the space environment, to entry into the atmosphere of Earth or one of Earth's planetary neighbors. Thermal control has been and remains a prime design concern for all spacecraft. Although many noteworthy advances in thermal control technology can be cited, such as advanced thermal coatings, louvered space radiators, low-temperature phase-change material packages, heat pipes and thermal diodes, and computational thermal analysis techniques, new and more challenging problems continue to arise. The prospects are for increased, not diminished, demands on the skill and ingenuity of the thermal control engineer and for continued advancement in those fundamental discipline areas upon which he relies. It is hoped that these volumes will be useful references for those working in these fields who may wish to bring themselves up-to-date in the applications to spacecraft and a guide and inspiration to those who, in the future, will be faced with new and, as yet, unknown design challenges.

Volume 69—361 pp., 6 × 9, illus., \$22.00 Mem., \$37.50 List
Volume 70—393 pp., 6 × 9, illus., \$22.00 Mem., \$37.50 List

TO ORDER WRITE: Publications Dept., AIAA, 1290 Avenue of the Americas, New York, N.Y. 10104